NIST Technical Note 1879

Tensile Properties of Commercially Pure, High-Purity and Ultra-High-Purity Iron: Results of an International Round-Robin

Enrico Lucon
Kenji Abiko
Marlies Lambrecht
Birgit Rehmer

This publication is available free of charge from:
http://dx.doi.org/10.6028/NIST.TN.1879

NIST
National Institute of Standards and Technology
U.S. Department of Commerce

NIST Technical Note 1879

Tensile Properties of Commercially Pure, High-Purity and Ultra-High-Purity Iron: Results of an International Round-Robin

Enrico Lucon
Applied Chemicals and Materials Division
Material Measurement Laboratory

Kenji Abiko
Institute for Material Research, Tohoku University
Sendai, Japan

Marlies Lambrecht
Structural Materials Tests, Belgian Nuclear Research Center, SCK•CEN
Mol, Belgium

Birgit Rehmer
BAM 5.2, Experimental and Model Based Mechanical Behaviour of Materials
Berlin, Germany

This publication is available free of charge from:
http://dx.doi.org/10.6028/NIST.TN.1879

April 2015

U.S. Department of Commerce
Penny Pritzker, Secretary

National Institute of Standards and Technology
Willie May, Acting Under Secretary of Commerce for Standards and Technology and Acting Director

Certain commercial entities, equipment, or materials may be identified in this document in order to describe an experimental procedure or concept adequately. Such identification is not intended to imply recommendation or endorsement by the National Institute of Standards and Technology, nor is it intended to imply that the entities, materials, or equipment are necessarily the best available for the purpose.

National Institute of Standards and Technology Technical Note 1879
Natl. Inst. Stand. Technol. Tech. Note 1879, 36 pages (April 2015)
CODEN: NTNOEF

This publication is available free of charge from:
http://dx.doi.org/10.6028/NIST.TN.1879

Abstract

The room temperature tensile properties of iron with different purity levels (commercially pure, high-purity, and ultra-high-purity) were characterized at different strain rates in the framework of an international Round-Robin involving four laboratories (BAM, IMR-TU, NIST, and SCK•CEN). The test results were collected and analyzed by NIST, and are presented in this Technical Note. Data from all the participating laboratories were found in good agreement, thus allowing a clear assessment of the influence of strain rate and purity level on tensile properties (mechanical resistance and ductility). A clear increase of yield strength and, to a lesser extent, tensile strength was observed for all materials as strain rate increases and purity level decreases. The highest strain rate sensitivity was associated with the highest purity level (ultra-high-purity Fe). Ductility trends were less unequivocal, but typically an increase of elongation at fracture and reduction of area was detected as strain rate and purity level increase. Significant differences in tensile properties were observed between the two investigated types of high-purity Fe, which can be attributed to an influence of the production process in terms of melting environment (atmosphere and crucible), as well as differences in chemical compositions.

Keywords

Commercially pure iron; ductility; high-purity iron; purity level; Round-Robin; strain rate; tensile strength; ultra-high-purity iron; yield strength.

Table of Contents

1. Round-Robin description

An interlaboratory comparison (aka Round-Robin) was conducted among four international laboratories for the characterization of the room temperature tensile properties of Fe with different degrees of purity, ranging from commercial purity (CP) to ultra-high purity (UHP). The purpose of this Round-Robin was to investigate the influence of purity level and strain rate on the tensile properties of iron.

The laboratories that participated in the Round-Robin are listed in Table 1, along with the names of the scientists who were responsible for testing and reporting results. The participants' data were collected and compared by NIST, Boulder CO (USA) in consultation with the participating institutes.

Table 1 - Round-Robin participants.

Institute	Location	Responsible
BAM	Berlin (Germany)	B. Rehmer
IMR-TU	Sendai (Japan)	K. Abiko
NIST	Boulder, CO (USA)	E. Lucon
SCK•CEN	Mol (Belgium)	M. Lambrecht

Four types of iron were tensile tested: commercially pure (CP) Fe, two types of high purity (HP) Fe, and ultra-high purity (UHP) Fe. The designations of the four types of pure Fe were K05 (CP), K02 (HP), S11 (HP), and A11 (UHP). Their impurity content, measured by the Institute of Material Research at Tohoku University (IMR-TU), is provided in Table 2.

Table 2 – Impurity content (weight ppm) of the investigated materials. (nm = not measured.)

Element	CP Fe	HP Fe		UHP Fe
	K05	K02	S11	A11
Fe	bal	bal	bal	bal
C	14.0	1.6	0.3	0.5
N	1.8	4	1.5	<0.1
O	8.6	60	72.1	8.3
S	1.1	0.9	12.2	1.2
H	nm		<0.1	<0.1
Al	75.0	3.0	nm	nm
B	10.9	2.6	nm	nm
Cr	nm	2.3	nm	nm
Mn	nm	1.3	nm	nm
Ni	nm	6.3	nm	<1
P	49	1	nm	nm
Si	nm	1	2	<1

Adding up the impurity contents in Table 2, the following purity levels are obtained:

- K05 (CP): 99.98396 %;
- K02 (HP): 99.9916 %;
- S11 (HP): 99.99118 %;
- A11 (UHP): 99.9999878 %.

The materials K05 and K02 were melted in argon atmosphere at 200 Torr (26.7 MPa) pressure, in a ceramics crucible (URC). S11 and A11 were melted in ultra-high vacuum (UHV, 10^{-7} Pa), by use of a water-cooled copper crucible.

From the scientific point of view, the most interesting material is A11 (electrolytic UHP iron). It was obtained by use of an induction melting furnace, located at IMR-TU in Sendai (Japan). The furnace is capable of melting iron ingots up to 10 kg, and its main chamber can be evacuated to a base pressure of 6.7×10^{-8} Pa. UHP Fe is used for the fundamental research on the intrinsic properties of iron and to determine the inherent effects of each impurity [1-3].

For each material, participants received tensile specimens of the geometry shown in Figure 1, which corresponds to the ASTM E8/E8M-13a Small-Size Round Specimen (Type 4). The specimens were manufactured and distributed by IMR-TU (Prof. Abiko).

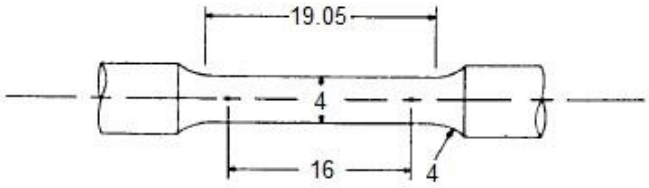

Figure 1 - Geometry of the tensile specimens tested for the Round-Robin (dimensions in mm).

For every material, each laboratory was required to test three specimens at three different strain rates, *i.e.*, 9 specimens per material, for a total of 36 specimens. Tests were to be conducted at room temperature (21 °C ± 3 °C) in accordance with ASTM E8/E8M-13a. As much as possible, an extensometer was required to be used to monitor specimen elongation. Due to miscommunication among participants, participating labs didn't all test at the same nominal strain rates. A summary of the tests performed is provided in the test matrix shown in Table 3.

The following parameters were reported by participants[1]:

- Yield strength[2], σ_{YS} (MPa);
- Tensile strength, σ_{TS} (MPa);
- Elongation at fracture, ε_t (%);
- Reduction of area, RA (%).

[1] Participants also reported uniform elongation ε_u (%). However, three of the four labs estimated ε_u from actuator displacement rather than specimen elongation. This parameter was therefore not included in the analyses.

[2] In case of discontinuous yielding, the minimum between the strength at an offset of 0.2 % plastic deformation ($\sigma_{p0.2}$) and the lower yield strength (σ_{LYS}) was reported as the yield strength for the test.

Table 3 - Test matrix for the Round-Robin.

Participant	Material	No. of tests	Strain rate (s^{-1})	Remarks
BAM	K05	3 3 3	10^{-3} 10^{-4} 10^{-5}	Tests were conducted with an extensometer which was removed at approximately 1 mm elongation.
	K02	3 3 3	10^{-3} 10^{-4} 10^{-5}	
	S11	3 3 3	10^{-3} 10^{-4} 10^{-5}	
	A11	3 3 3	10^{-3} 10^{-4} 10^{-5}	
IMR-TU	K05	3 3 3	5×10^{-3} 5×10^{-4} 5×10^{-5}	
	K02	3 3 3	5×10^{-3} 5×10^{-4} 5×10^{-5}	
	S11	3 3 3	5×10^{-3} 5×10^{-4} 5×10^{-5}	
	A11	3 3 3	5×10^{-3} 5×10^{-4} 10^{-5}	
NIST	K05	3 3 3	10^{-3} 10^{-4} 10^{-5}	Tests were conducted with an extensometer which was removed at approximately 0.7 mm elongation.
	K02	3 3 4	10^{-3} 10^{-4} 10^{-5}	
	S11	3 3 3	10^{-3} 10^{-4} 10^{-5}	
	A11	3 3 3	10^{-3} 10^{-4} 10^{-5}	
SCK•CEN	K05	2 1 2 1 2 1	10^{-3} 5×10^{-3} 10^{-4} 5×10^{-4} 5×10^{-4} 10^{-5}	Tests at 5×10^{-3} s^{-1}, 5×10^{-4} s^{-1}, and 5×10^{-5} s^{-1} were conducted without extensometer. The remaining tests were conducted with an extensometer which was removed at approximately 5-6 mm elongation.
	K02	2 1 2 1 2 1	10^{-3} 5×10^{-3} 10^{-4} 5×10^{-4} 5×10^{-4} 10^{-5}	
	S11	2 1 2 1 2 1	10^{-3} 5×10^{-3} 10^{-4} 5×10^{-4} 5×10^{-4} 10^{-5}	
	A11	2 1 2 1 2 1	10^{-3} 5×10^{-3} 10^{-4} 5×10^{-4} 5×10^{-4} 10^{-5}	

2. Results of the individual participants

2.1. BAM results

The test results reported by BAM [4] are presented in Table 4.

Table 4 - Test results reported by BAM [4].

Material	Specimen ID	Strain rate (s^{-1})	σ_{YS} (MPa)	σ_{TS} (MPa)	ε_t (%)	RA (%)
CP Fe	K05-1_19	1E-03	228	288	45	95
	K05-1_20	1E-03	233	281	48	95
	K05-1_21	1E-03	232	280	47	95
	K05-2_21	1E-04	211	264	49	95
	K05-2_22	1E-04	200	260	51	96
	K05-2_23	1E-04	202	262	53	96
	K05-3_19	1E-05	DATA ACQUISITION FAILED		48	95
	K05-3_20	1E-05	178	250	50	95
	K05-3_21	1E-05	174	250	52	95
HP Fe	K02-1_21	1E-03	198	252	44	86
	K02-1_22	1E-03	192	242	45	86
	K02-1_23	1E-03	194	241	48	91
	K02-2_19	1E-04	189	250	40	88
	K02-2_20	1E-04	159	232	49	91
	K02-2_21	1E-04	158	229	54	89
	K02-3_21	1E-05	184	237	39	91
	K02-3_22	1E-05	163	230	44	92
	K02-3_23	1E-05	163	230	46	91
	S11-1_9	1E-03	111	208	73	97
	S11-1_10	1E-03	99	205	73	96
	S11-1_11	1E-03	106	205	72	96
	S11-2_28	1E-04	89	200	72	94
	S11-2_29	1E-04	87	201	74	96
	S11-2_30	1E-04	91	203	74	97
	S11-1_28	1E-05	66	190	64	95
	S11-1_29	1E-05	64	189	65	96
	S11-1_30	1E-05	63	188	68	96
UHP Fe	A11-1_17	1E-03	68	200	67	95
	A11-1_18	1E-03	68	201	74	95
	A11-1_19	1E-03	69	201	73	96
	A11-2_17	1E-04	43	189	65	95
	A11-2_18	1E-04	44	186	65	94
	A11-2_19	1E-04	44	188	71	96
	A11-3_23	1E-05	27	179	71	95
	A11-3_24	1E-05	28	178	66	96
	A11-3_25	1E-05	29	177	37	95

Average values of all tensile parameters are presented as a function of tested material in Table 5 and as a function of strain rate in Table 6. Average values are also illustrated in Figures 2 to 6.

Table 5 – Average BAM test results as a function of tested material.

Material	Strain rate (s^{-1})	σ_{YS} (MPa)	σ_{TS} (MPa)	ε_t (%)	RA (%)
K05	1E-03	231	283	47	95
	1E-04	204	262	51	95
	1E-05	176	250	50	95
K02	1E-03	195	245	46	88
	1E-04	169	237	47	89
	1E-05	163	232	43	91
S11	1E-03	105	206	73	96
	1E-04	88	201	73	96
	1E-05	66	189	66	96
A11	1E-03	68	201	71	95
	1E-04	44	188	67	95
	1E-05	28	178	58	95

Table 6 – Average BAM test results as a function of strain rate.

Strain rate (s^{-1})	Material	σ_{YS} (MPa)	σ_{TS} (MPa)	ε_t (%)	RA (%)
1E-03	K05	231	283	47	95
	K02	195	245	46	88
	S11	105	206	73	96
	A11	68	201	71	95
1E-04	K05	204	262	51	95
	K02	169	237	47	89
	S11	88	201	73	96
	A11	44	188	67	95
1E-05	K05	176	250	50	95
	K02	163	232	43	91
	S11	66	189	66	96
	A11	28	178	58	95

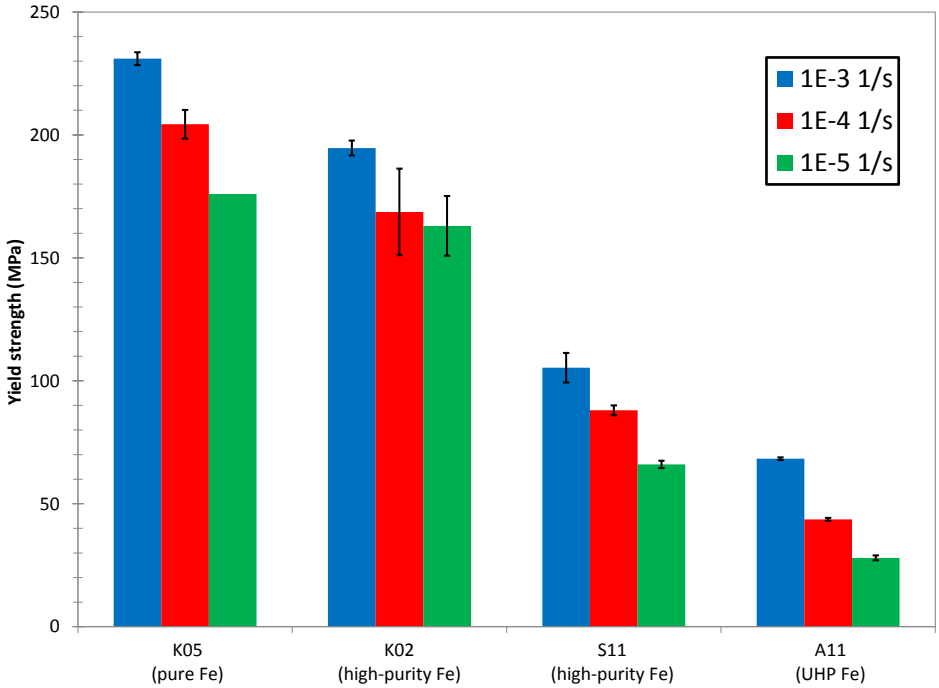

Figure 2 - Average values of yield strength measured by BAM. Error bars indicate standard deviations.

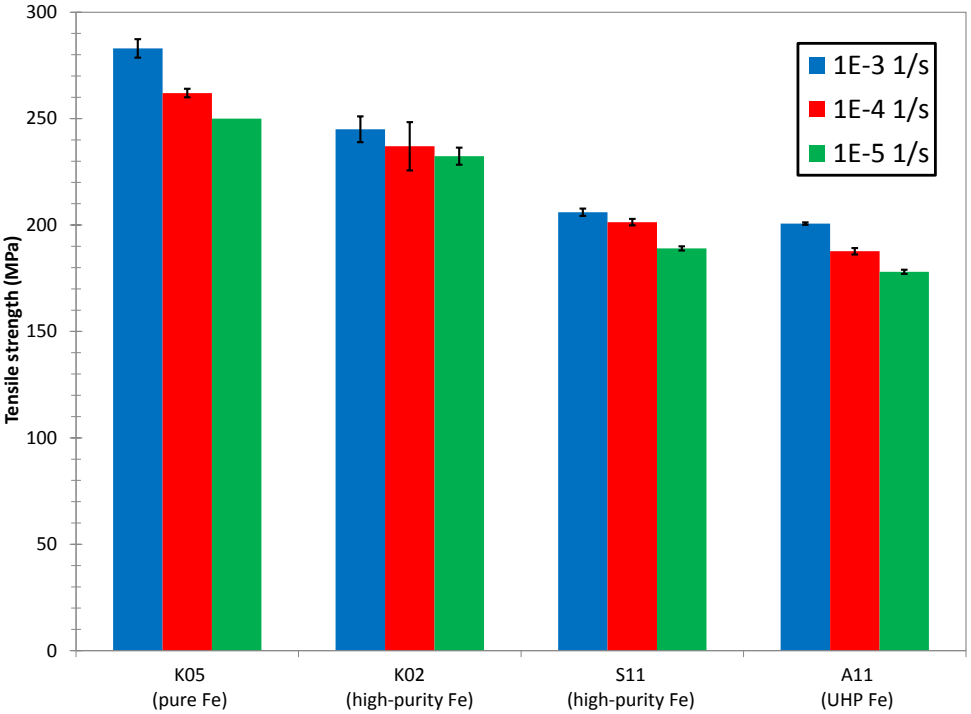

Figure 3 - Average values of tensile strength measured by BAM. Error bars indicate standard deviations.

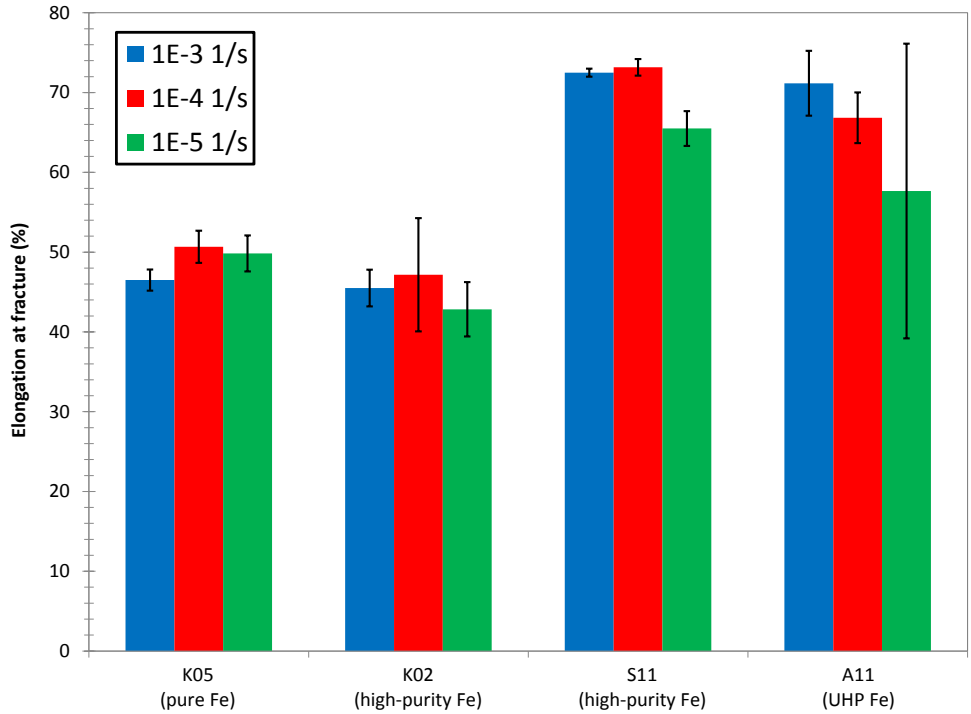

Figure 4 - Average values of elongation at fracture measured by BAM. Error bars indicate standard deviations.

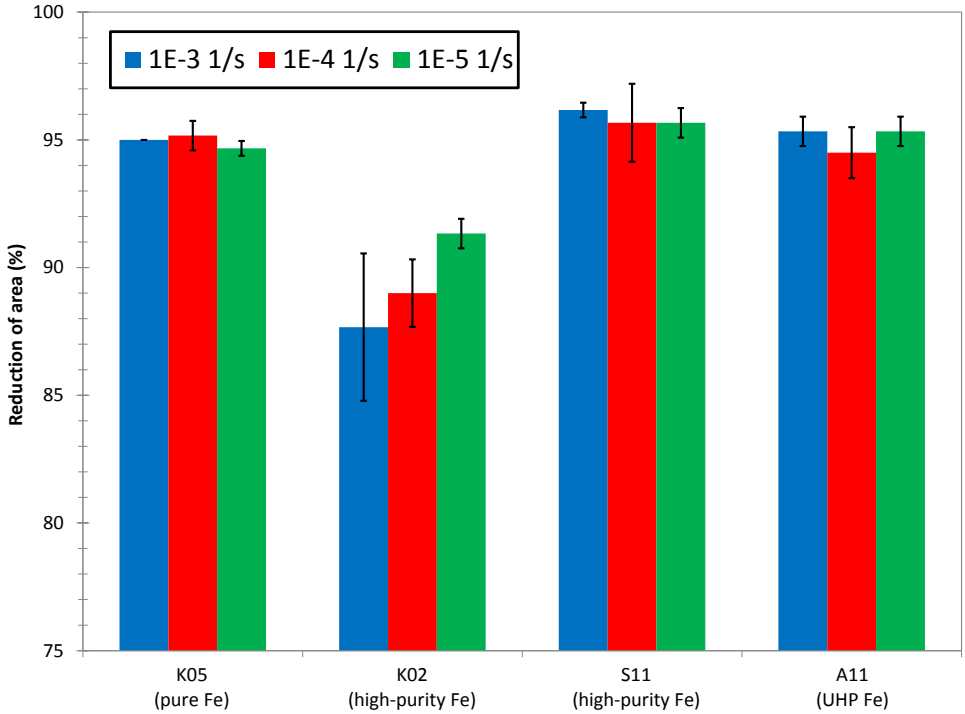

Figure 5 - Average values of reduction of area measured by BAM.

Very clear and consistent trends for yield and tensile strengths can be observed in Figures 2 and 3. Both parameters decrease as material purity increases and strain rate decreases. Specific trends are not detected in Figures 4 and 5 for ductility parameters (ε_t and *RA*).

2.2. IMR-TU results

The test results obtained by IMR-TU[3] are presented in Table 7. Note that reduction of area was not measured.

Table 7 - Test results obtained by IMR-TU.

Material	Specimen ID	Strain rate (s^{-1})	σ_{YS} (MPa)	σ_{TS} (MPa)	ε_t (%)
CP Fe	K05-1_29	5E-03	245	282	49
	K05-1_30	5E-03	243	280	48
	K05-1_31	5E-03	243	279	48
	K05-2_31	5E-04	199	257	54
	K05-2_32	5E-04	215	259	55
	K05-2_33	5E-04	210	259	52
	K05-3_29	5E-05	200	248	52
	K05-3_30	5E-05	201	248	52
	K05-3_31	5E-05	201	255	50
HP Fe	K02-1_31	5E-03	211	247	47
	K02-1_32	5E-03	204	243	57
	K02-1_33	5E-03	200	239	55
	K02-2_29	5E-04	189	241	45
	K02-2_30	5E-04	187	240	44
	K02-2_31	5E-04	183	237	51
	K02-3_31	5E-05	171	235	45
	K02-3_32	5E-05	175	235	41
	K02-3_33	5E-05	176	239	41
	S11-1_12	5E-03	126	211	77
	S11-1_13	5E-03	123	210	70
	S11-1_14	5E-03	124	212	71
	S11-2_25	5E-04	106	207	73
	S11-2_26	5E-04	98	205	72
	S11-2_27	5E-04	99	206	69
	S11-1_25	5E-05	71	FILE INCOMPLETE	
	S11-1_26	5E-05	67	188	66
	S11-1_27	5E-05	70	187	62
UHP Fe	A11-1_27	5E-03	92	199	68
	A11-1_29	5E-03	91	198	70
	A11-1_30	5E-03	94	201	68
	A11-2_27	5E-03	56	184	68
	A11-2_28	5E-03	59	189	70
	A11-2_29	5E-03	59	187	68
	A11-3_29	5E-03	41	175	67
	A11-3_30	5E-03	44	178	67
	A11-3_31	5E-03	42	177	62

Average values of all tensile parameters are presented as a function of tested material in Table 8 and as a function of strain rate in Table 9. Average values are also illustrated in Figures 6 to 8.

[3] IMR-TU provided raw test data to NIST, who analyzed the tests and calculated the results.

Table 8 – Average IMR-TU test results as a function of tested material.

Material	Strain rate (s^{-1})	σ_{YS} (MPa)	σ_{TS} (MPa)	ε_t (%)
K05	5E-03	244	280	48
	5E-04	208	258	53
	5E-05	201	251	51
K02	5E-03	205	243	53
	5E-04	187	239	47
	5E-05	174	236	42
S11	5E-03	124	211	73
	5E-04	101	206	71
	5E-05	70	188	64
A11	5E-03	92	199	69
	5E-04	58	187	68
	5E-05	42	177	65

Table 9 – Average IMR-TU test results as a function of strain rate.

Strain rate (s^{-1})	Material	σ_{YS} (MPa)	σ_{TS} (MPa)	ε_t (%)
5E-03	K05	244	280	48
	K02	205	243	53
	S11	124	211	73
	A11	92	199	69
5E-04	K05	208	258	53
	K02	187	239	47
	S11	101	206	71
	A11	58	187	68
5E-05	K05	201	251	51
	K02	174	236	42
	S11	70	188	64
	A11	42	177	65

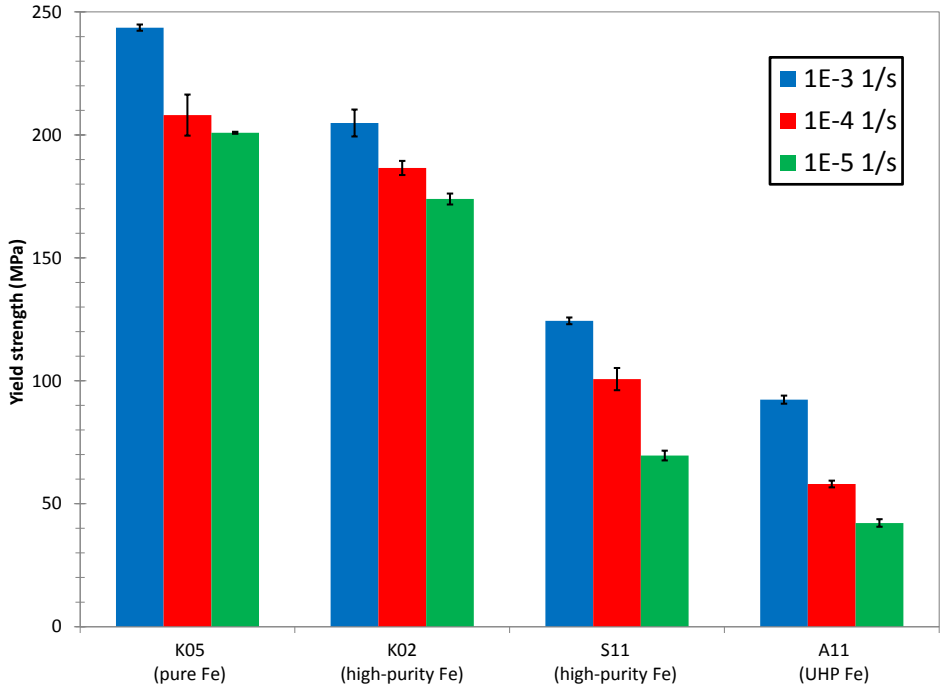

Figure 6 - Average values of yield strength measured by IMR-TU. Error bars indicate standard deviations.

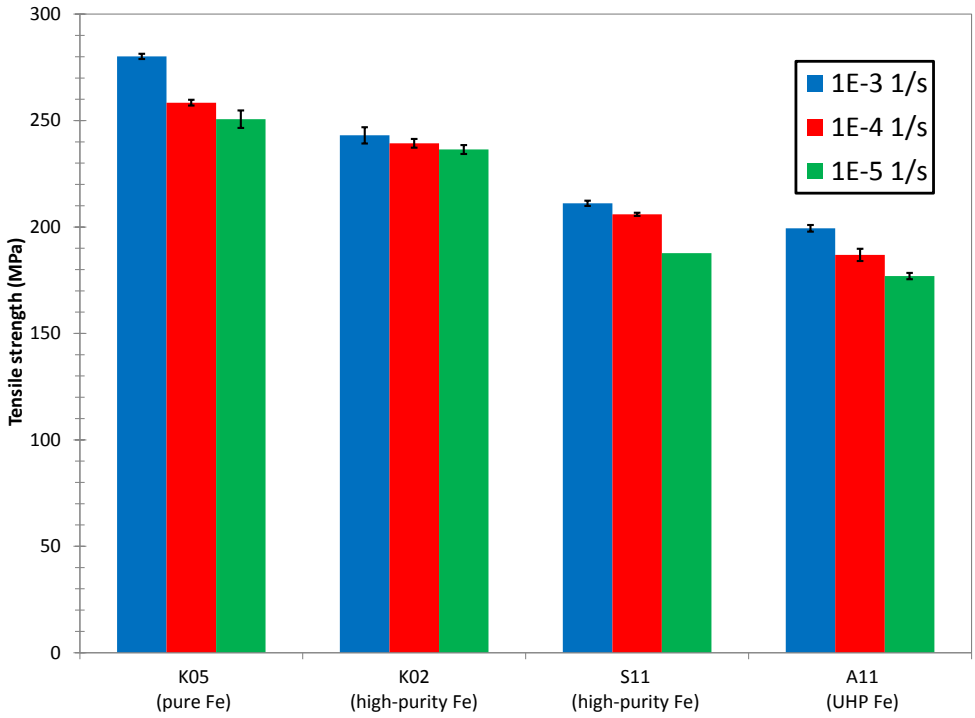

Figure 7 - Average values of tensile strength measured by IMR-TU. Error bars indicate standard deviations.

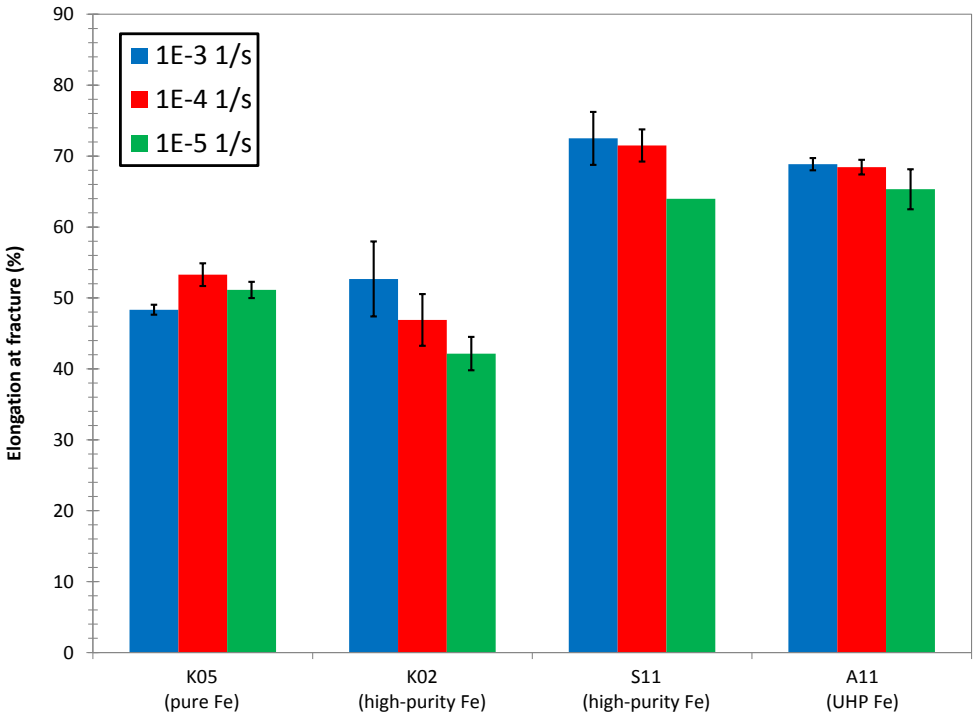

Figure 8 - Average values of elongation at fracture measured by IMR-TU. Error bars indicate standard deviations.

The observed trends for yield and tensile strengths (Figures 6 and 7) are similar to the BAM results shown in Figures 2 and 3: strength decreases with increasing material purity and decreasing strain rate.

2.3. NIST results

The test results obtained by NIST are presented in Table 10. Note that a fourth K02 specimen was tested at 10^{-5} s^{-1} because of the anomalous results yielded by specimen K02-3_30.

Table 10 - Test results reported by NIST.

Material	Specimen ID	Strain rate (s^{-1})	σ_{YS} (MPa)	σ_{TS} (MPa)	ε_t (%)	RA (%)
P Fe	K05-1_26	1E-03	219	277	58	96
	K05-1_27	1E-03	229	282	62	96
	K05-1_28	1E-03	243	294	51	96
	K05-2_16	1E-04	197	264	53	96
	K05-2_28	1E-04	220	271	62	96
	K05-2_30	1E-04	213	271	55	96
	K05-3_15	1E-05	172	253	50	95
	K05-3_27	1E-05	179	259	52	95
	K05-3_28	1E-05	205	267	51	95
HP Fe	K02-1_28	1E-03	183	243	61	92
	K02-1_29	1E-03	185	246	54	90
	K02-1_30	1E-03	202	256	48	91
	K02-2_26	1E-04	150	233	59	91
	K02-2_27	1E-04	148	231	57	93
	K02-2_28	1E-04	186	253	51	91
	K02-2_14	1E-05	131	218	42	92
	K02-3_28	1E-05	139	224	52	94
	K02-3_29	1E-05	137	223	51	93
	K02-3_30	1E-05	177	244	42	92
	S11-1_15	1E-03	103	219	71	97
	S11-1_17	1E-03	109	219	67	96
	S11-1_22	1E-03	109	220	67	96
	S11-2_22	1E-04	92	212	67	95
	S11-2_23	1E-04	94	214	76	96
	S11-2_24	1E-04	94	216	63	97
	S11-1_16	1E-05	64	194	61	96
	S11-1_23	1E-05	71	196	64	95
	S11-1_24	1E-05	76	197	61	97
UHP Fe	A11-1_24	1E-03	78	214	70	97
	A11-1_25	1E-03	74	208	73	96
	A11-1_26	1E-03	76	211	65	94
	A11-2_24	1E-04	53	197	67	96
	A11-2_25	1E-04	52	197	70	96
	A11-2_26	1E-04	48	194	65	93
	A11-3_20	1E-05	39	183	80	93
	A11-3_21	1E-05	37	184	68	93
	A11-3_22	1E-05	38	187	59	93

Figure 9 compares force/actuator displacement curves for the K02 (HP iron) specimens tested at the lowest strain rate (10^{-5} s^{-1}). The outlier behavior of specimen K02-3_30 is evident, with higher strength and lower ductility than the other three specimens. No apparent reason for this anomaly could be identified. However, we should also note that similar situations were also observed at 10^{-3} s^{-1} and 10^{-4} s^{-1}, in reference to specimens K02-1_30 and K02-2_28 respectively.

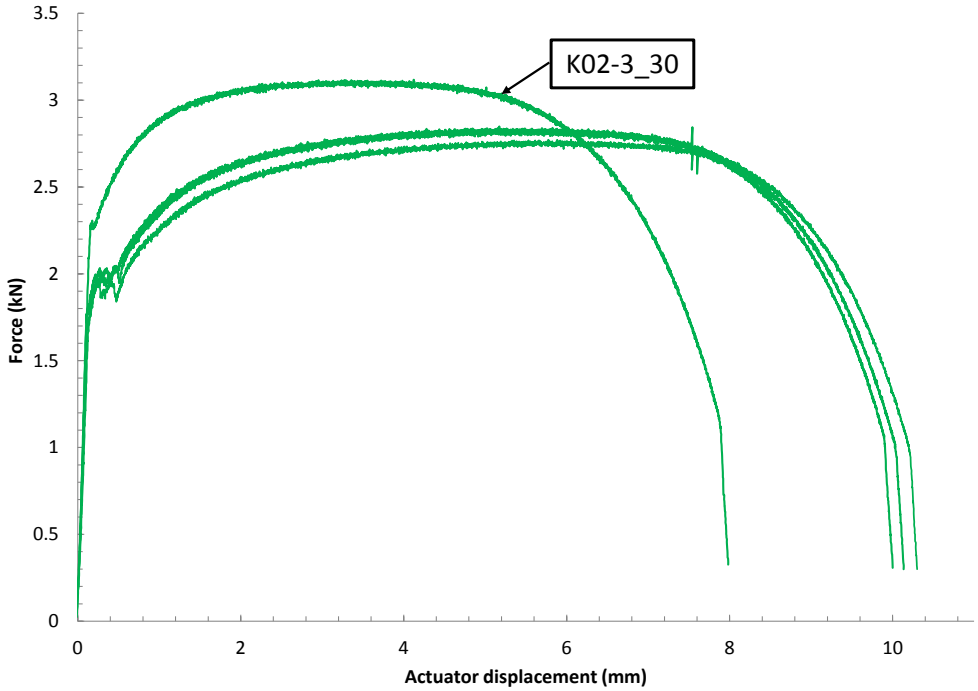

Figure 9 - Comparison between K02 specimens tested by NIST at 10^{-5} s^{-1}.

Average values for all tensile parameters are presented as a function of tested material in Table 11 and as a function of strain rate in Table 12. Average values and standard deviations (indicated by error bars) are also illustrated in Figures 10 to 13.

Table 11 – Average NIST test results as a function of tested material.

Material	Strain rate (s^{-1})	σ_{YS} (MPa)	σ_{TS} (MPa)	ε_t (%)	RA (%)
K05	1E-03	231	284	57	96
	1E-04	210	269	57	96
	1E-05	185	260	51	95
K02	1E-03	190	248	54	91
	1E-04	161	239	56	92
	1E-05	132	228	47	93
S11	1E-03	107	219	68	96
	1E-04	93	214	69	96
	1E-05	71	196	62	96
A11	1E-03	76	211	69	96
	1E-04	51	196	67	95
	1E-05	38	185	69	93

Table 12 – Average NIST test results as a function of strain rate.

Strain rate (s^{-1})	Material	σ_{YS} (MPa)	σ_{TS} (MPa)	ε_t (%)	RA (%)
1E-03	K05	231	284	57	96
	K02	190	248	54	91
	S11	107	219	68	96
	A11	76	211	69	96
1E-04	K05	210	269	57	96
	K02	161	239	56	92
	S11	93	214	69	96
	A11	51	196	67	95
1E-05	K05	185	260	51	95
	K02	132	228	47	93
	S11	71	196	62	96
	A11	38	185	69	93

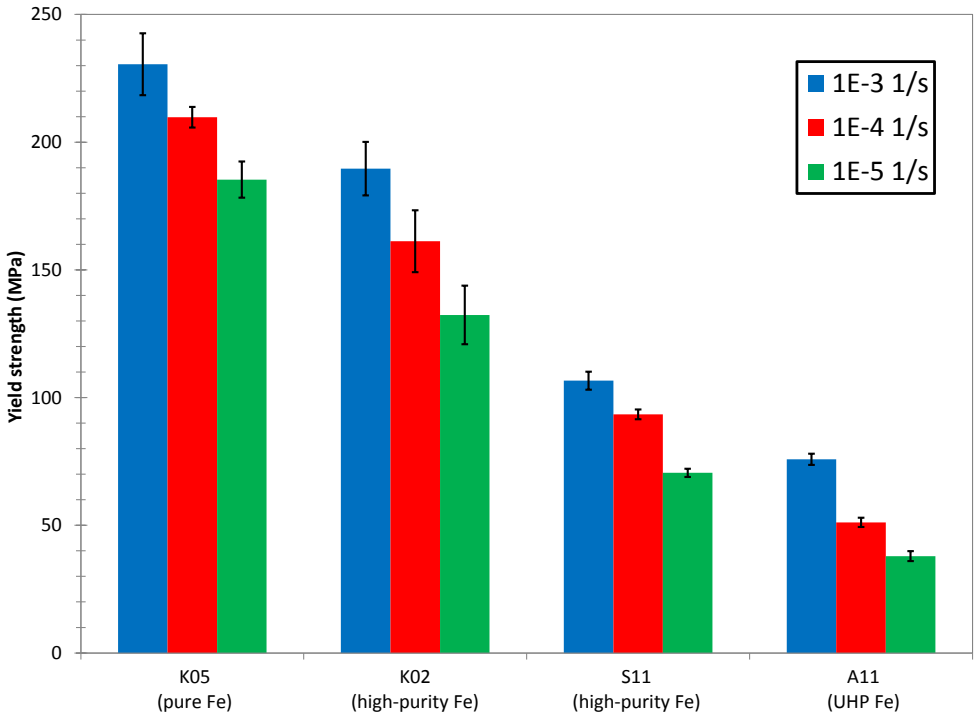

Figure 10 - Average values of yield strength measured by NIST. Error bars indicate standard deviations.

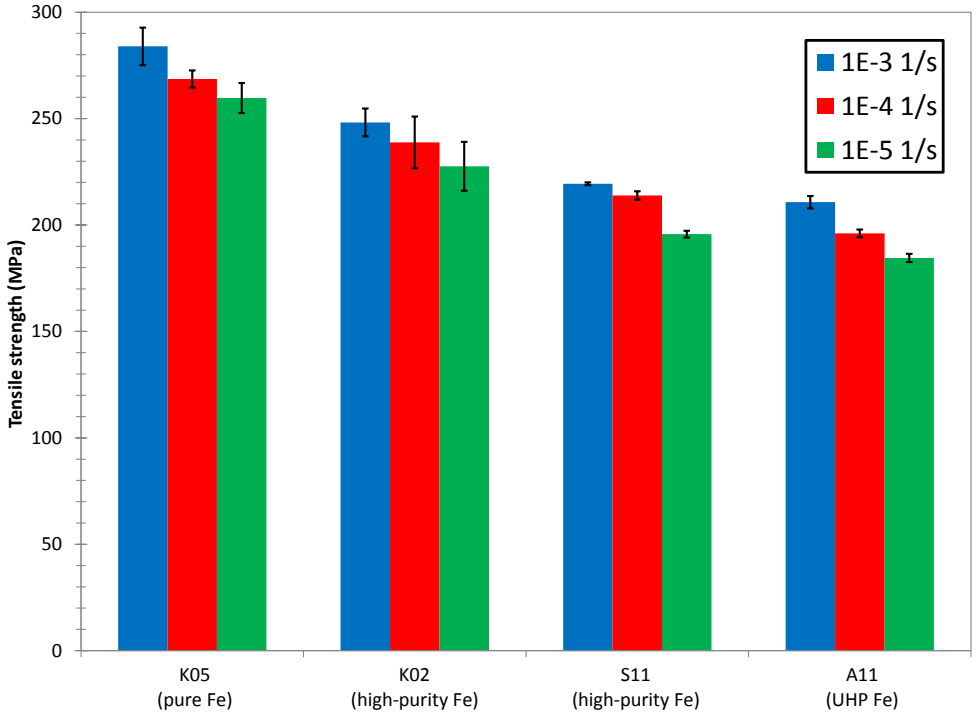

Figure 11 - Average values of tensile strength measured by NIST. Error bars indicate standard deviations.

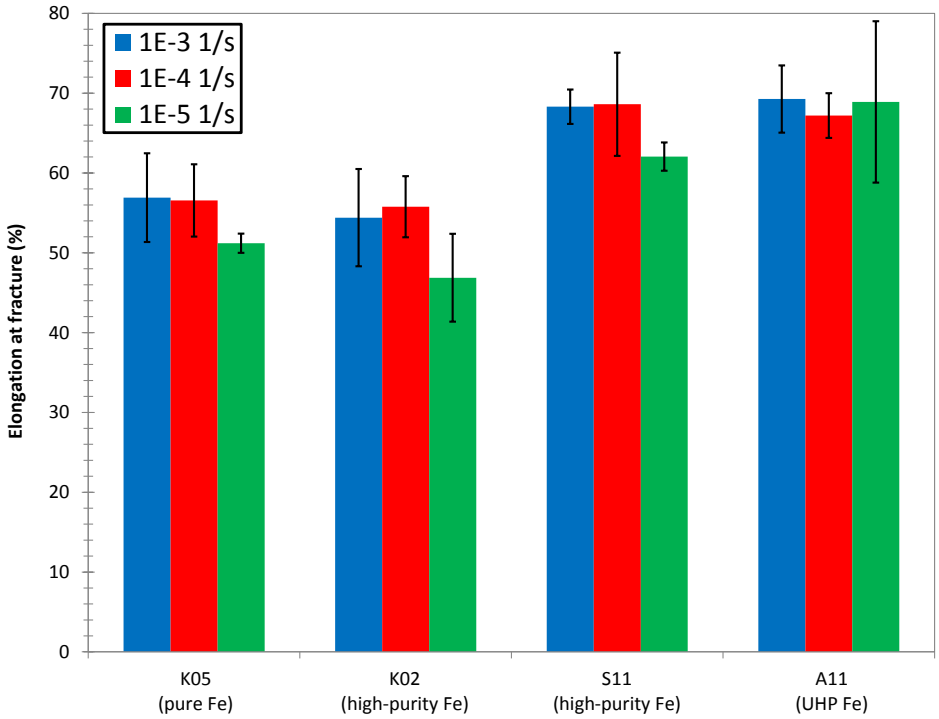

Figure 12 - Average values of elongation at fracture measured by NIST. Error bars indicate standard deviations.

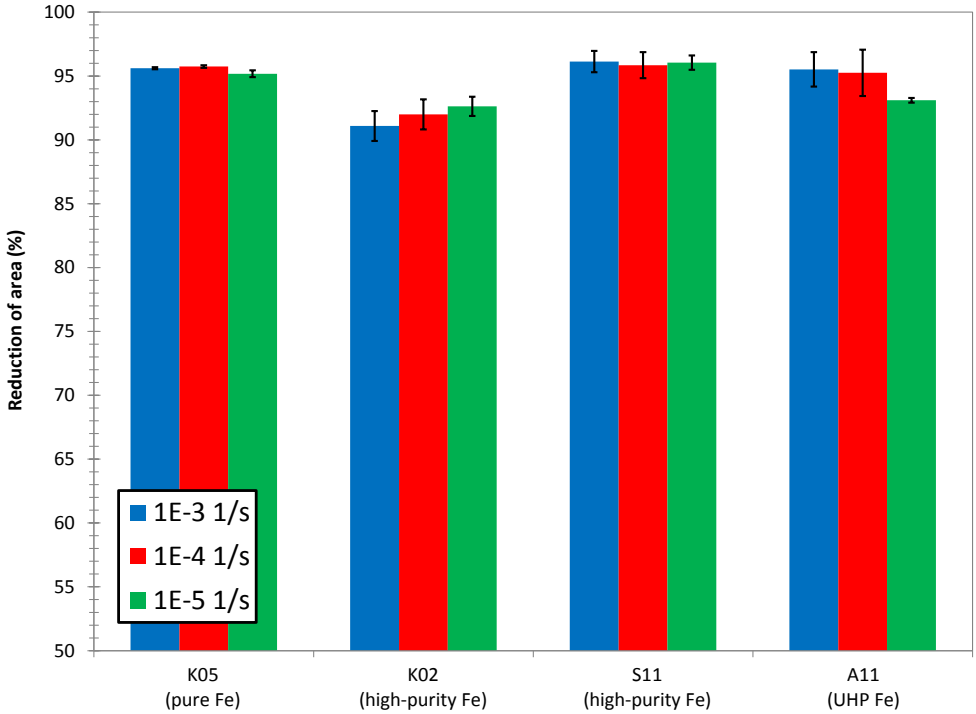

Figure 13 - Average values of reduction of area measured by NIST. Error bars indicate standard deviations.

As already observed for BAM and IMR-TU results, yield and tensile strength systematically decrease as the material purity increases and strain rate increases (Figures 10 and 11). Ductility parameters do not exhibit equally clear patterns.

2.4. SCK•CEN results

The test results obtained by SCK•CEN are presented in Table 13. For every test condition, specimens were tested at two strain rates (*e.g.*, 10^{-3} s^{-1} and 5×10^{-3} s^{-1}). The tests performed at 5×10^{-3} s^{-1}, 5×10^{-4} s^{-1}, and 5×10^{-5} s^{-1} were conducted without extensometer. For these tests, the parameter σ_{p02} was estimated from force and actuator displacement data, after linearization of the initial portion of the test record. For 9 of these 12 tests, σ_{YS} corresponds to σ_{LYS}, which is not affected by the use of actuator displacement or specimen elongation.

Table 13 - Test results obtained by SCK•CEN.

Material	Specimen ID	Strain rate (s^{-1})	σ_{YS} (MPa)	σ_{TS} (MPa)	ε_t (%)	RA (%)
CP Fe	K05-1_16	5E-03	250	292	51	94
	K05-1_17	1E-03	246	284	50	95
	K05-1_18	1E-03	244	293	47	96
	K05-2_18	5E-04	228	275	57	96
	K05-2_19	1E-04	215	265	53	96
	K05-2_20	1E-04	227	271	49	96
	K05-3_16	5E-05	195	257	57	94
	K05-3_17	1E-05	189	254	50	95
	K05-3_18	1E-05	193	256	50	94
HP Fe	K02-1_18	5E-03	224	262	50	91
	K02-1_19	1E-03	194	246	50	92
	K02-1_20	1E-03	208	257	46	90
	K02-2_16	5E-04	201	253	49	88
	K02-2_17	1E-04	185	244	47	91
	K02-2_18	1E-04	202	261	38	88
	K02-3_18	5E-05	177	242	52	92
	K02-3_19	1E-05	167	234	48	91
	K02-3_20	1E-05	187	250	40	92
	S11-1_6	5E-03	145	229	71	97
	S11-1_7	1E-03	111	218	68	97
	S11-1_8	1E-03	111	218	71	97
	S11-2_31	5E-04	117	221	76	96
	S11-2_32	1E-04	93	208	70	97
	S11-2_33	1E-04	96	209	70	95
	S11-1_31	5E-05	75	203	68	96
	S11-1_32	1E-05	67	195	62	97
	S11-1_33	1E-05	71	197	65	97
	S11-3_23	1E-05	114	210	61	93
UHP Fe	A11-1_14	5E-03	107	215	80	96
	A11-1_15	1E-03	72	204	72	97
	A11-1_16	1E-03	72	204	71	94
	A11-2_14	5E-04	71	206	75	97
	A11-2_15	1E-04	52	195	68	96
	A11-2_16	1E-04	49	194	68	96
	A11-3_26	5E-05	44	188	68	94
	A11-3_27	1E-05	38	180	65	94
	A11-3_28	1E-05	39	181	65	95

Average values of all tensile parameters (considering only tests conducted at 10^{-3} s^{-1}, 10^{-4} s^{-1}, and 10^{-5} s^{-1}) are presented as a function of tested material in Table 14 and as a function of strain rate in Table 15. Average values are also illustrated in Figures 14 to 17.

Table 14 – Average SCK•CEN test results as a function of tested material.

Material	Strain rate (s^{-1})	σ_{YS} (MPa)	σ_{TS} (MPa)	ε_t (%)	RA (%)
K05	1E-03	245	289	49	96
	1E-04	221	268	51	96
	1E-05	191	255	50	95
K02	1E-03	201	252	48	91
	1E-04	194	253	43	90
	1E-05	177	242	44	92
S11	1E-03	111	218	70	97
	1E-04	95	209	70	96
	1E-05	84	201	63	96
A11	1E-03	72	204	72	96
	1E-04	51	195	68	96
	1E-05	39	181	65	95

Table 15 – Average SCK•CEN test results as a function of strain rate.

Strain rate (s^{-1})	Material	σ_{YS} (MPa)	σ_{TS} (MPa)	ε_t (%)	RA (%)
1E-03	K05	245	289	49	96
	K02	201	252	48	91
	S11	111	218	70	97
	A11	72	204	72	96
1E-04	K05	221	268	51	96
	K02	194	253	43	90
	S11	95	209	70	96
	A11	51	195	68	96
1E-05	K05	191	255	50	95
	K02	177	242	44	92
	S11	84	201	63	96
	A11	39	181	65	95

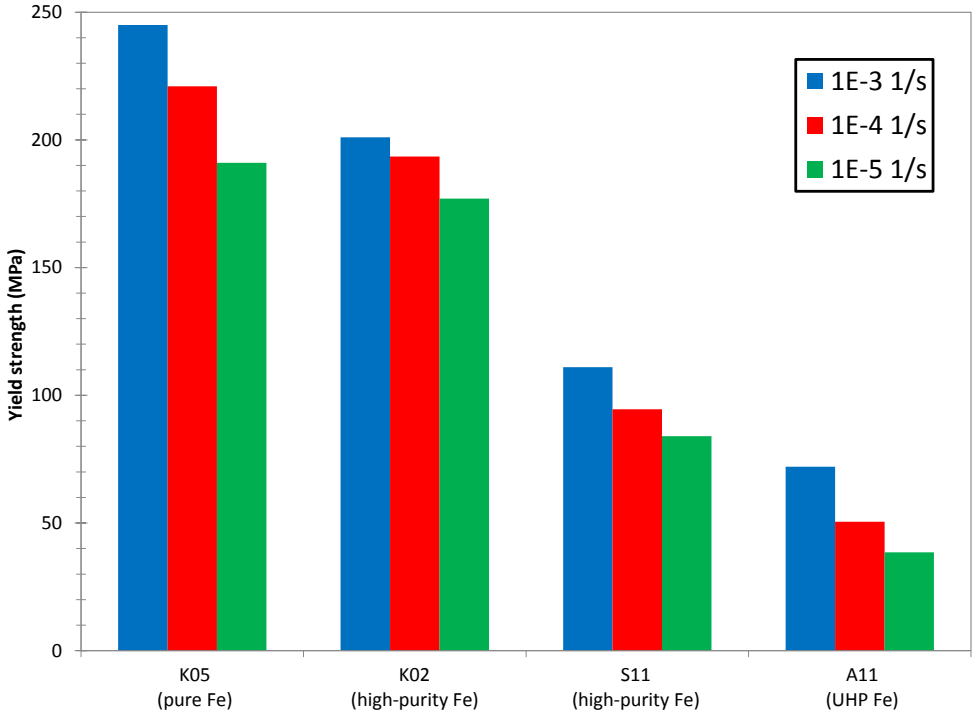

Figure 14 - Average values of yield strength measured by SCK•CEN.

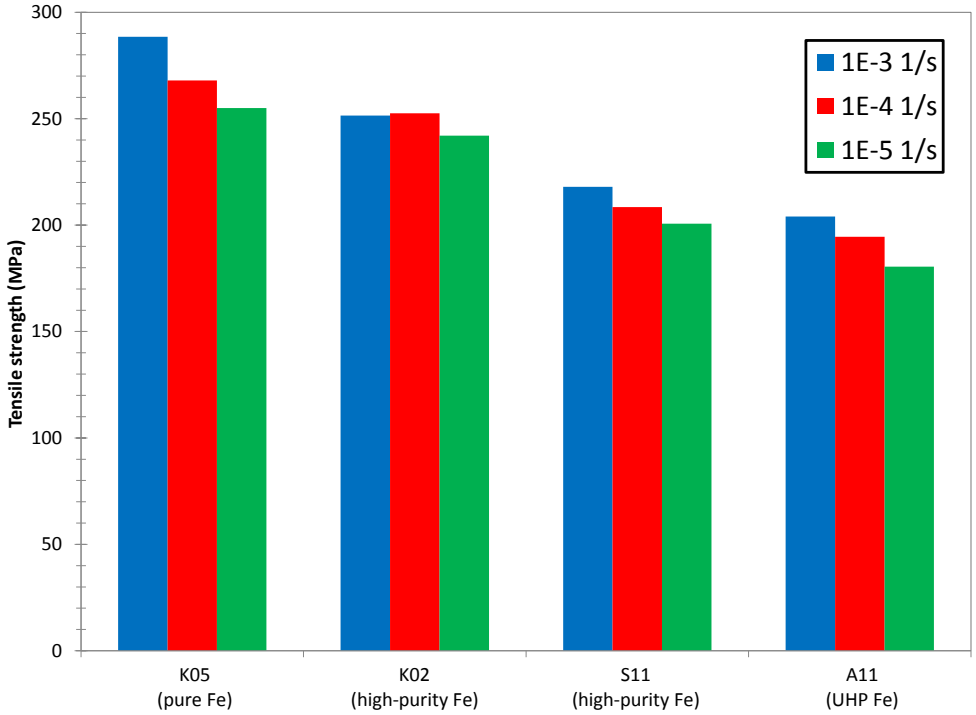

Figure 15 - Average values of tensile strength measured by SCK•CEN.

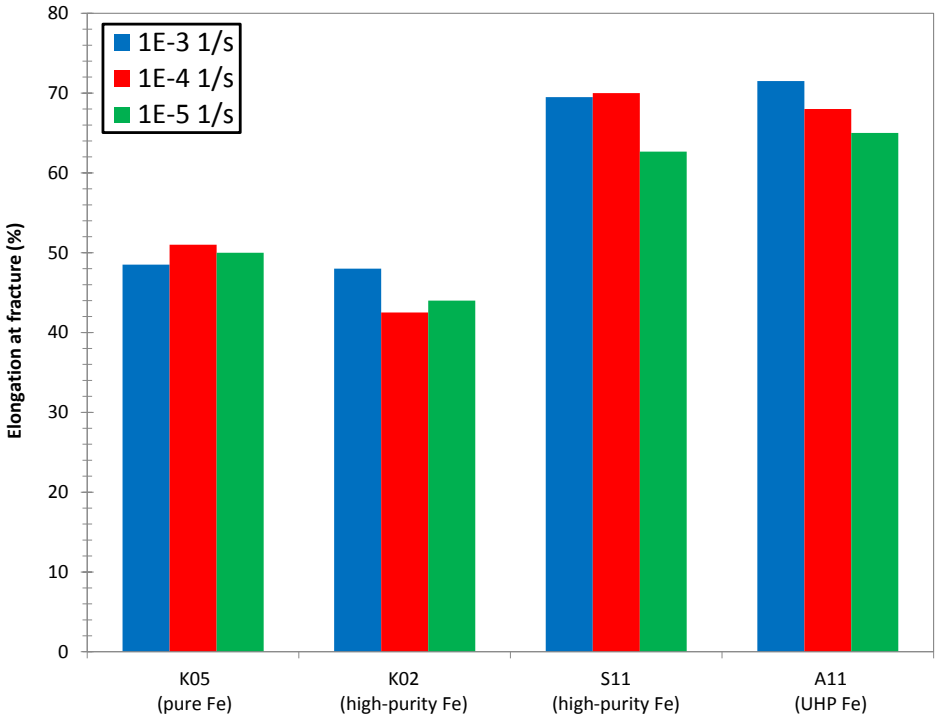

Figure 16 - Average values of elongation at fracture measured by SCK•CEN.

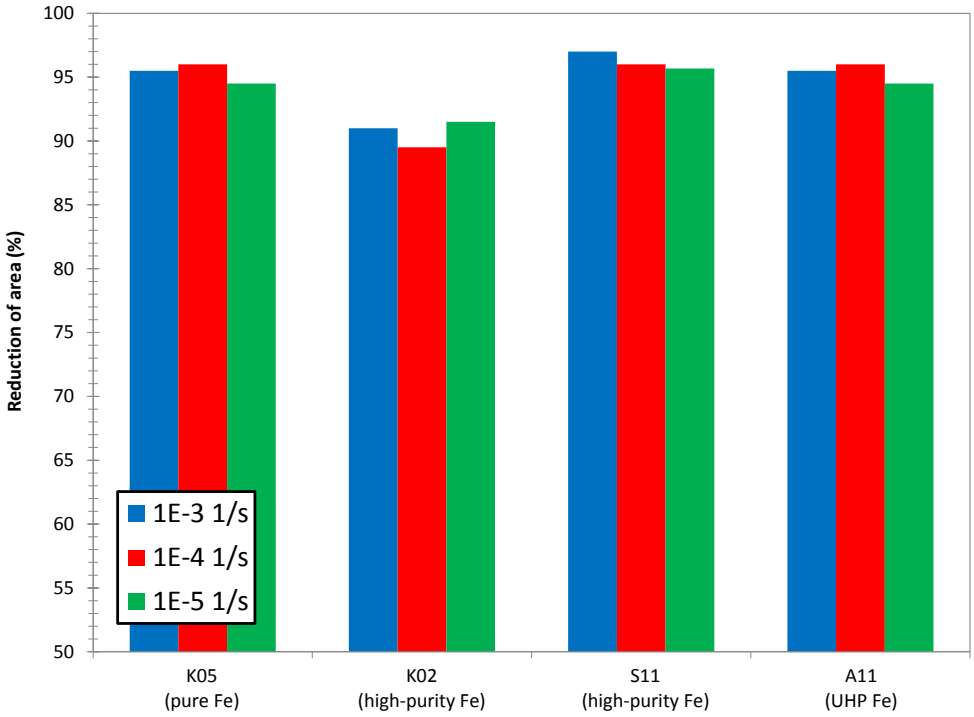

Figure 17 - Average values of reduction of area measured by SCK•CEN.

Similar to the other participants, the results obtained by SCK•CEN confirm that yield and tensile strengths decrease with increasing material purity and decreasing strain rate, whereas ductility parameters do not exhibit specific trends.

3. Comparison of participants' data

Table 16 is the master table which presents all the test results provided by the Round-Robin participants. When multiple tests on the same material and at the same strain rate are available for a single participant, the corresponding average values are given in Table 16.

Table 16 – Master table of the tensile Round-Robin results.

Material	Institute	Strain rate (s^{-1})	σ_{YS} (MPa)	σ_{TS} (MPa)	ε_t (%)	RA (%)
K05	BAM	1E-03	231	283	47	95
	NIST	1E-03	231	284	57	96
	SCK-CEN	1E-03	245	289	49	96
	IMR-TU	5E-03	244	280	48	
	SCK-CEN	5E-03	250	292	51	94
	BAM	1E-04	204	262	51	95
	NIST	1E-04	210	269	57	96
	SCK-CEN	1E-04	221	268	51	96
	IMR-TU	5E-04	208	258	53	
	SCK-CEN	5E-04	228	275	57	96
	BAM	1E-05	176	250	50	95
	NIST	1E-05	185	260	51	95
	SCK-CEN	1E-05	191	255	50	95
	IMR-TU	5E-05	201	251	51	
	SCK-CEN	5E-05	195	257	57	94
K02	BAM	1E-03	195	245	46	88
	NIST	1E-03	190	248	54	91
	SCK-CEN	1E-03	201	252	48	91
	IMR-TU	5E-03	205	243	53	
	SCK-CEN	5E-03	224	262	50	91
	BAM	1E-04	169	237	47	89
	NIST	1E-04	161	239	56	92
	SCK-CEN	1E-04	194	253	43	90
	IMR-TU	5E-04	187	239	47	
	SCK-CEN	5E-04	201	253	49	88
	BAM	1E-05	163	232	43	91
	NIST	1E-05	132	228	47	93
	SCK-CEN	1E-05	177	242	44	92
	IMR-TU	5E-05	174	236	42	
	SCK-CEN	5E-05	177	242	52	92
S11	BAM	1E-03	105	206	73	96
	NIST	1E-03	107	219	68	96
	SCK-CEN	1E-03	111	218	70	97
	IMR-TU	5E-03	124	211	73	
	SCK-CEN	5E-03	145	229	71	97
	BAM	1E-04	88	201	73	96
	NIST	1E-04	93	214	69	96
	SCK-CEN	1E-04	95	209	70	96
	IMR-TU	5E-04	101	206	71	
	SCK-CEN	5E-04	117	221	76	96
	BAM	1E-05	66	189	66	96
	NIST	1E-05	71	196	62	96
	SCK-CEN	1E-05	84	201	63	96
	IMR-TU	5E-05	70	188	64	
	SCK-CEN	5E-05	75	203	68	96
A11	BAM	1E-03	68	201	71	95
	NIST	1E-03	76	211	69	96
	SCK-CEN	1E-03	72	204	72	96
	IMR-TU	5E-03	92	199	69	
	SCK-CEN	5E-03	107	215	80	96
	BAM	1E-04	44	188	67	95
	NIST	1E-04	51	196	67	95
	SCK-CEN	1E-04	51	195	68	96
	IMR-TU	5E-04	58	187	68	
	SCK-CEN	5E-04	71	206	75	97
	BAM	1E-05	28	178	58	95
	NIST	1E-05	38	185	69	93
	SCK-CEN	1E-05	39	181	65	95
	IMR-TU	5E-05	42	177	65	
	SCK-CEN	5E-05	44	188	68	94

3.1. Yield strength

The values of yield strength obtained by BAM, NIST and SCK•CEN at 10^{-3} s^{-1}, 10^{-4} s^{-1}, and 10^{-5} s^{-1} are illustrated in Figure 18. Yield strengths measured by IMR-TU and SCK•CEN at 5×10^{-3} s^{-1}, 5×10^{-4} s^{-1}, and 5×10^{-5} s^{-1} are shown in Figure 19.

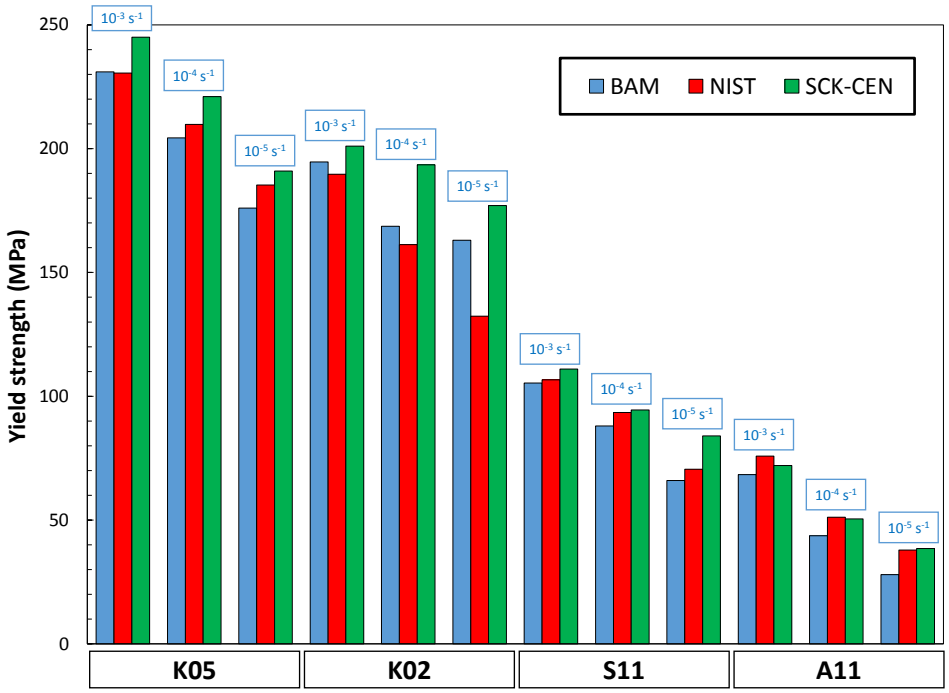

Figure 18 – Yield strength values measured at 10^{-3} s^{-1}, 10^{-4} s^{-1}, and 10^{-5} s^{-1}.

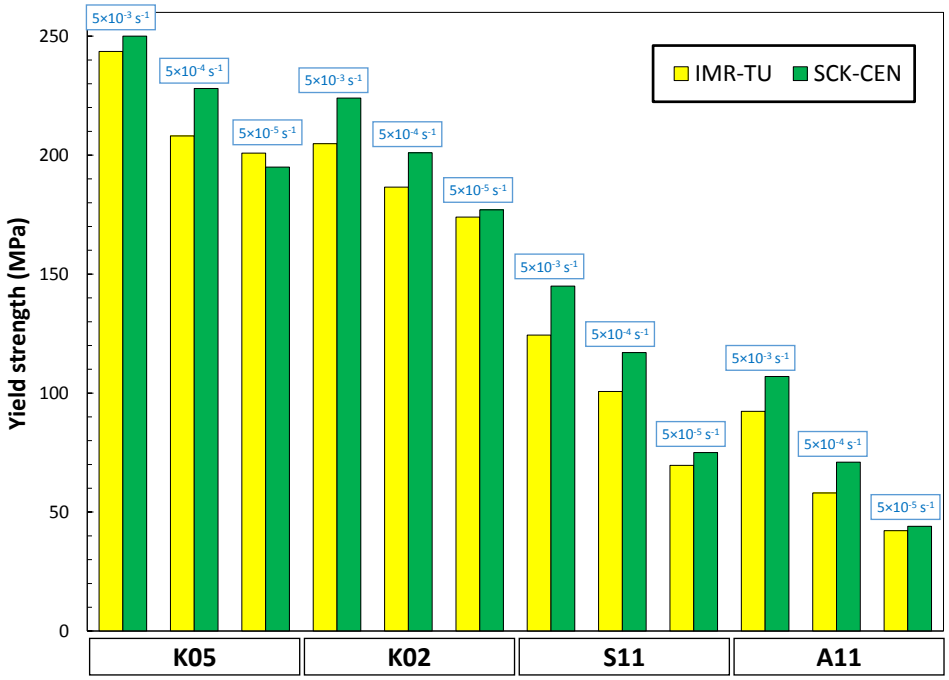

Figure 19 – Yield strength values measured at 5×10^{-3} s^{-1}, 5×10^{-4} s^{-1}, and 5×10^{-5} s^{-1}.

3.2. Tensile strength

The values of tensile strength obtained by BAM, NIST and SCK•CEN at 10^{-3} s^{-1}, 10^{-4} s^{-1}, and 10^{-5} s^{-1} are illustrated in Figure 20. Tensile strengths measured by IMR-TU and SCK•CEN at 5×10^{-3} s^{-1}, 5×10^{-4} s^{-1}, and 5×10^{-5} s^{-1} are shown in Figure 21.

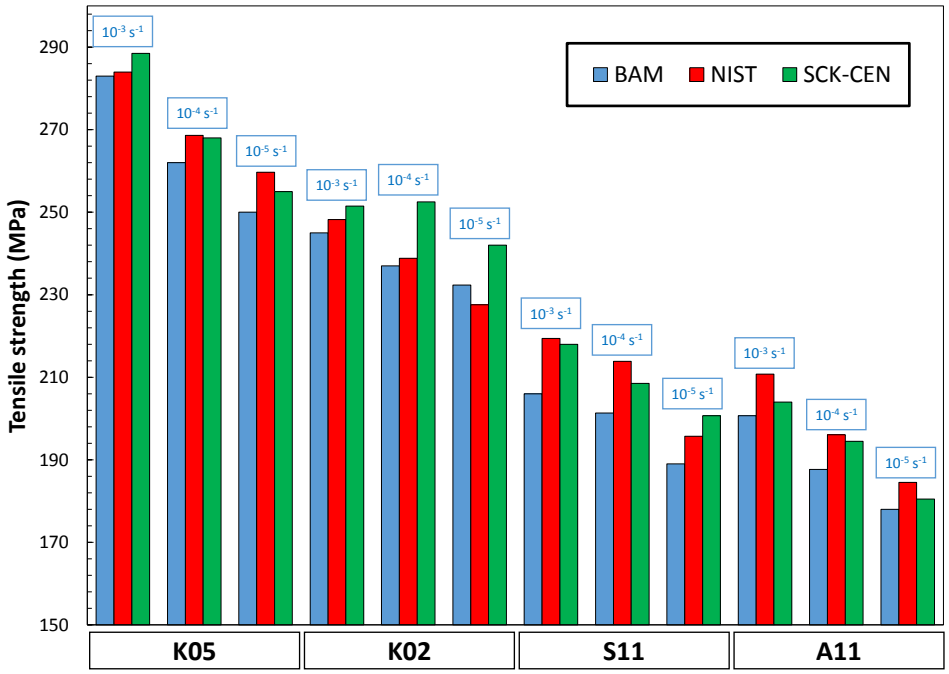

Figure 20 – Tensile strength values measured at 10^{-3} s^{-1}, 10^{-4} s^{-1}, and 10^{-5} s^{-1}.

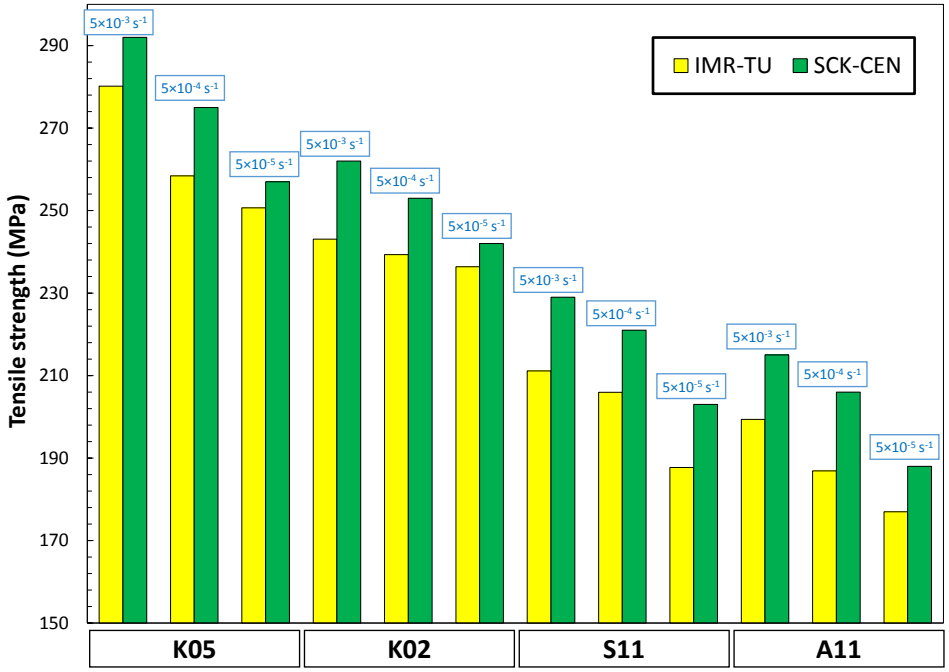

Figure 21 – Tensile strength values measured at 5×10^{-3} s^{-1}, 5×10^{-4} s^{-1}, and 5×10^{-5} s^{-1}.

3.3. Elongation at fracture

The values of elongation at fracture obtained by BAM, NIST and SCK•CEN at 10^{-3} s^{-1}, 10^{-4} s^{-1}, and 10^{-5} s^{-1} are illustrated in Figure 22. Values measured by IMR-TU and SCK•CEN at 5×10^{-3} s^{-1}, 5×10^{-4} s^{-1}, and 5×10^{-5} s^{-1} are shown in Figure 23.

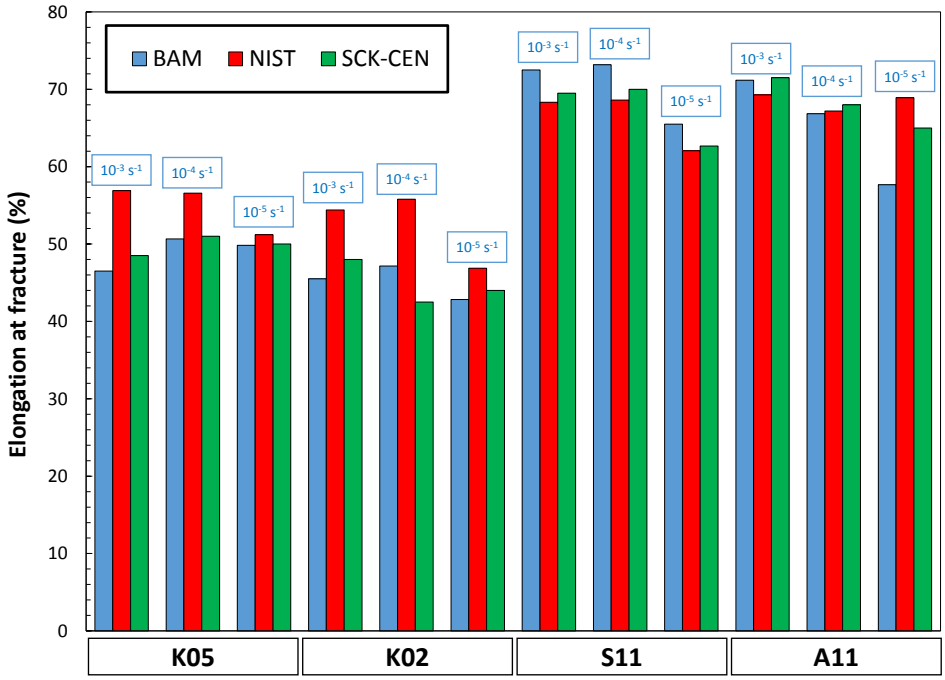

Figure 22 – Elongation at fracture values measured at 10^{-3} s^{-1}, 10^{-4} s^{-1}, and 10^{-5} s^{-1}.

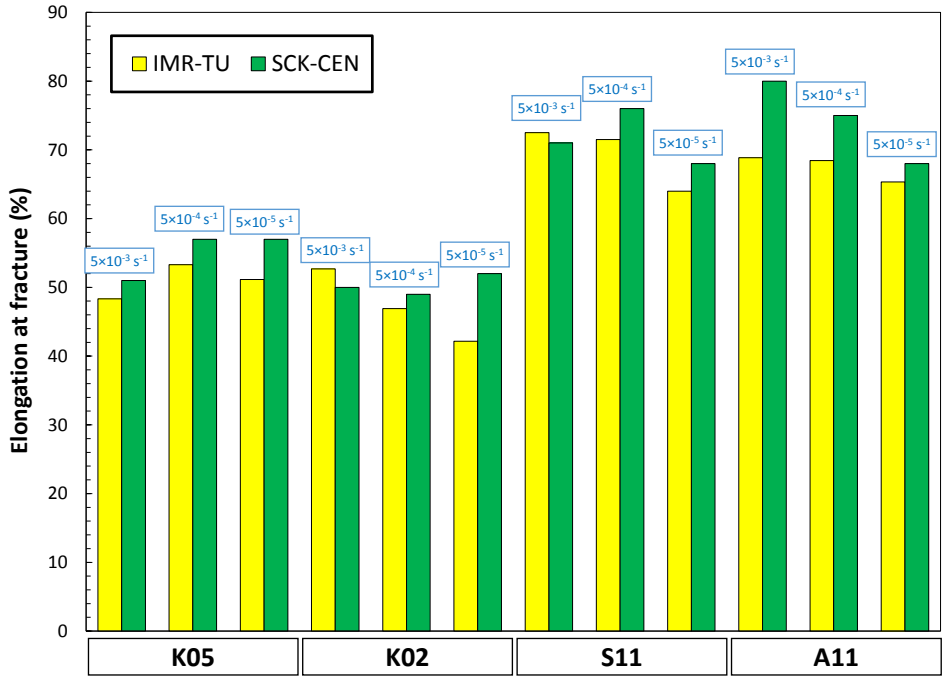

Figure 23 – Elongation at fracture values measured at 5×10^{-3} s^{-1}, 5×10^{-4} s^{-1}, and 5×10^{-5} s^{-1}.

3.4. Reduction of area

The values of reduction of area obtained by BAM, NIST and SCK•CEN at 10^{-3} s^{-1}, 10^{-4} s^{-1}, and 10^{-5} s^{-1} are illustrated in Figure 24.

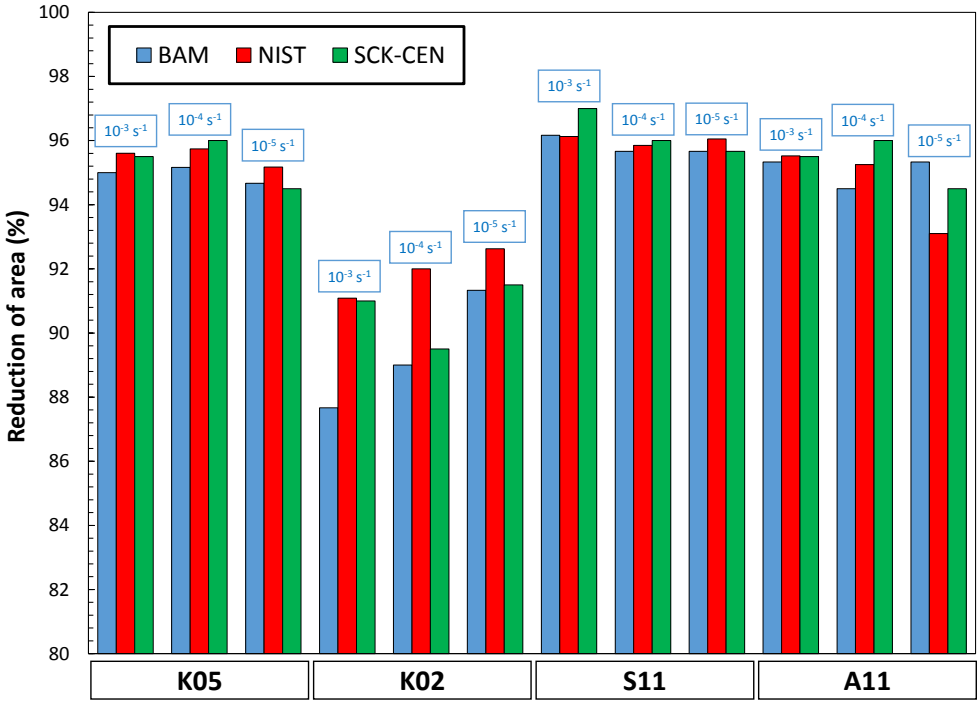

Figure 24 – Reduction of area values measured at 10^{-3} s^{-1}, 10^{-4} s^{-1}, and 10^{-5} s^{-1}.

3.5. General remarks

The comparisons presented in the previous sections show a tendency for SCK•CEN to measure higher yield strengths than the other participants (Figures 18 and 19). The same is observed in Figure 21 for tensile strengths with respect to IMR-TU.

No other trends can be detected from the examination of Figures 18 to 24.

4. Discussion

The tensile properties of the investigated materials, obtained by averaging the results provided by the Round-Robin participants, are presented in Table 17.

Table 17 - Average tensile properties of the investigated materials.

Material	Strain rate (s^{-1})	σ_{YS} (MPa)	σ_{TS} (MPa)	ε_t (%)	RA (%)
K05	1E-03	236	285	51	95
	5E-03	247	286	50	94
	1E-04	212	266	53	96
	5E-04	218	267	55	96
	1E-05	184	255	50	95
	5E-05	198	254	54	94
K02	1E-03	195	248	49	90
	5E-03	214	253	51	91
	1E-04	174	243	48	90
	5E-04	194	246	48	88
	1E-05	157	234	45	92
	5E-05	175	239	47	92
S11	1E-03	108	214	70	96
	5E-03	135	220	72	97
	1E-04	92	208	71	96
	5E-04	109	213	74	96
	1E-05	74	195	63	96
	5E-05	72	195	66	96
A11	1E-03	72	205	71	95
	5E-03	100	207	74	96
	1E-04	48	193	67	95
	5E-04	65	196	72	97
	1E-05	35	181	64	94
	5E-05	43	182	67	94

Standard deviations for yield and tensile strengths are provided in Table 18.

Table 18 – Standard deviations for yield and tensile strengths.

Material	Strain rate (s^{-1})	St. dev. (MPa) σ_{YS}	St. dev. (MPa) σ_{TS}
K05	1E-03	8.2	2.9
	5E-03	4.5	8.4
	1E-04	8.5	3.7
	5E-04	14.1	11.7
	1E-05	7.6	4.8
	5E-05	4.1	4.5
K02	1E-03	5.7	3.3
	5E-03	13.6	13.4
	1E-04	16.9	8.5
	5E-04	10.2	9.7
	1E-05	22.8	7.3
	5E-05	2.2	4.0
S11	1E-03	3.0	7.4
	5E-03	14.6	12.6
	1E-04	3.5	6.3
	5E-04	11.5	10.6
	1E-05	9.4	5.9
	5E-05	3.8	10.8
A11	1E-03	3.8	5.1
	5E-03	10.4	11.1
	1E-04	4.1	4.5
	5E-04	9.2	13.5
	1E-05	5.9	3.3
	5E-05	1.3	7.8

Tensile parameters, with the exception of uniform elongation, are represented in Figures 25 to 28 as a function of strain rate. The power law relationships obtained by least-square regression of the mean σ_{YS} and σ_{TS} values given in Table 17 have the following form:

$$\sigma = \alpha \left(\frac{d\varepsilon}{dt} \right)^{\beta} \quad , \tag{1}$$

where σ is yield or tensile strength in MPa, and $\left(\frac{d\varepsilon}{dt} \right)$ is strain rate in s^{-1}. The regression coefficients α and β are listed in Table 19 for the four materials, along with the coefficient of determination (R^2) of the regression. A power law is generally considered to provide the best description of the relationship between yield strength and strain rate at a given temperature [5]. The exponent β represents the material's strain rate sensitivity at the test temperature.

In Figures 27 and 28, elongation at fracture and reduction of area are also fitted by the use of power functions, just as a guide for the eye. However, trends are not clear and scatter is significant, so fitting coefficients for ductility parameters are not reported.

Table 19 - Regression results for yield and tensile strengths (average values).

Material	Designation	Parameter	α	β	R^2
CP Fe	K05	σ_{YS}	320.25	0.0476	0.9698
		σ_{TS}	321.14	0.0213	0.8356
HP Fe	K02	σ_{YS}	275.62	0.0479	0.9795
		σ_{TS}	269.88	0.0121	0.9869
	S11	σ_{YS}	229.81	0.1041	0.9163
		σ_{TS}	248.23	0.0213	0.8925
UHP Fe	A11	σ_{YS}	237.57	0.1702	0.9945
		σ_{TS}	237.89	0.0243	0.9170

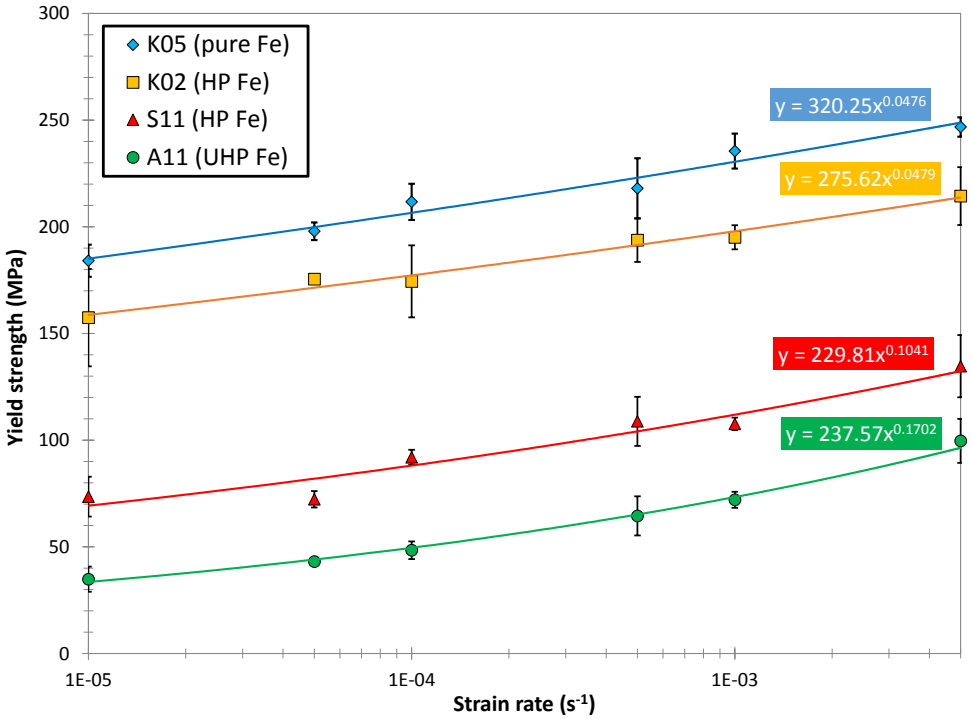

Figure 25 - Average yield strength values as a function of strain rate. Error bars correspond to one standard deviation.

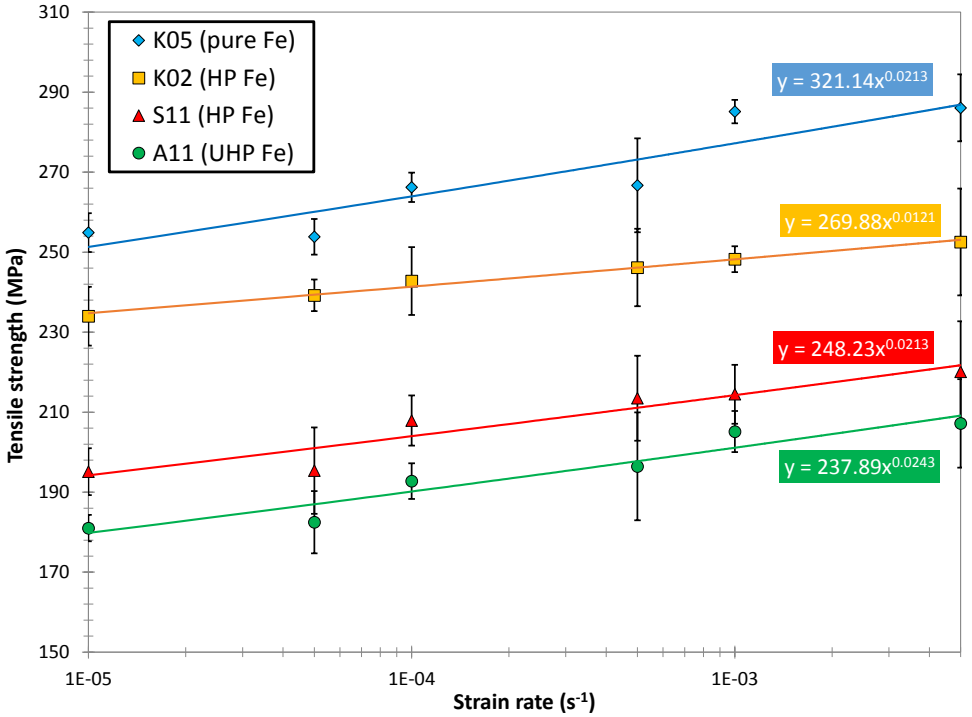

Figure 26 - Average tensile strength values as a function of strain rate. Error bars correspond to one standard deviation.

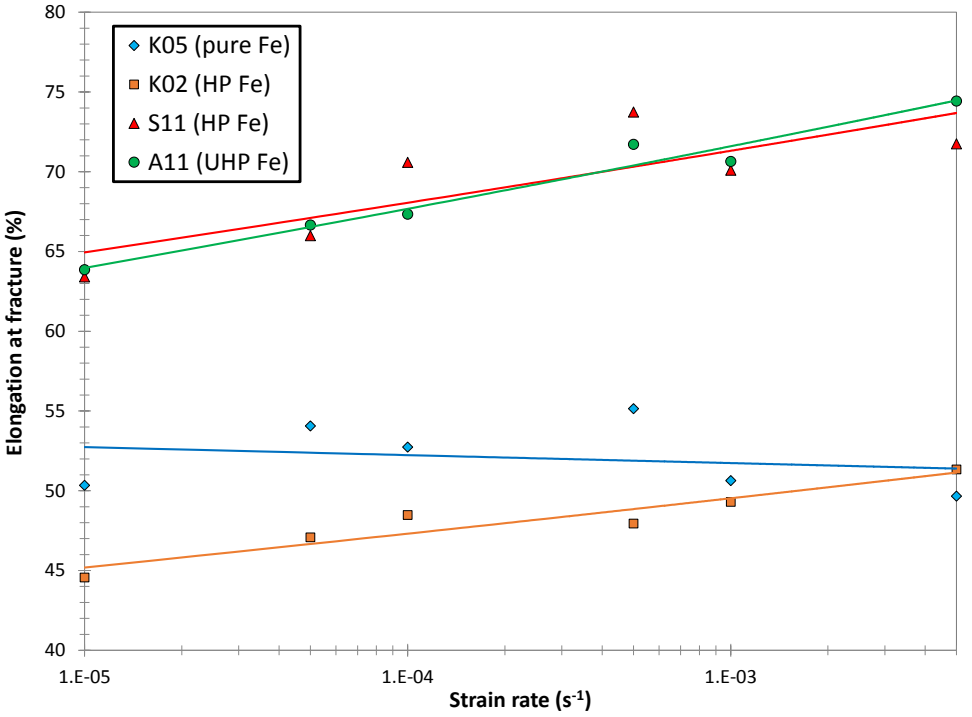

Figure 27 - Average elongation at fracture values as a function of strain rate.

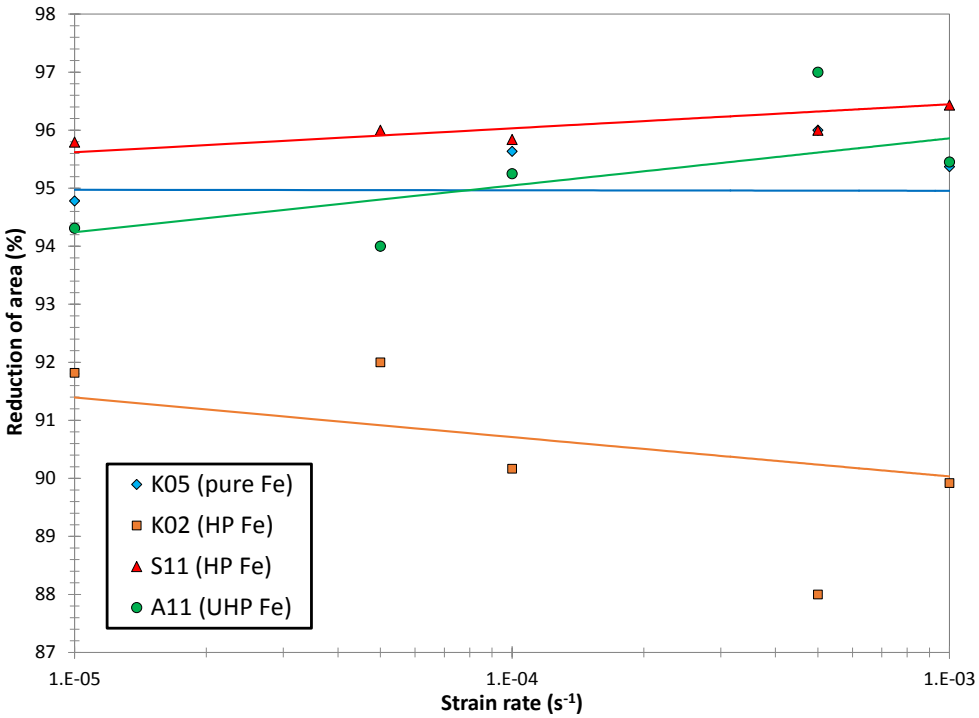

Figure 28 - Average reduction of area values as a function of strain rate.

Examination of Figures 25 and 26 confirms the well-documented increase of yield and tensile strength with increasing strain rates [6-9]. The strain rate sensitivity, expressed by the coefficient β in Table 19, increases with material purity, and is maximum for A11 (UHP iron). Note also that the strain rate sensitivity of CP Fe (K05) and HP Fe (K02) is almost identical.

The influence of strain rate on tensile strengths (Figure 26) is smaller than for yield strengths, more so for the higher purity materials (Table 19). Once again, the coefficient β is highest for A11 (UHP iron). In this case, K05 (CP Fe) and S11 (HP Fe) yielded identical values of β.

As already mentioned, trends for ductility parameters (elongation at fracture in Figure 27 and reduction of area in Figure 28) are less clear. Generally, ductility appears to increase with strain rate, with a few exceptions.

Strengthening mechanisms in iron typically include precipitation, as well as interstitial and solid-solution strengthening. As the purity of iron increases, the mechanical resistance (yield and tensile strength) decreases because of a cleaner microstructure which offers less resistance to the movement of dislocations. Trends for elongation at fracture and reduction of area are somewhat less well-defined. The effect of iron purity level on tensile properties can be appreciated in Figures 25 to 28, but also in Figures 18 to 24 and Table 17.

It is interesting to note that the Round-Robin results indicate a clear difference between the two materials classified as high-purity iron, K02 and S11. The former has mechanical properties which are relatively close to the commercially pure iron (K05), whereas the latter behaves very

similar to the ultra-high purity iron (A11). Differences in chemical composition, such as the significantly different contents of C, N, and S in Table 2, are certainly among the main causes of these observations. The effect of the melting environment (200 Torr argon in a ceramics crucible for K05 and K02; ultra-high vacuum in a water-cooled Cu crucible for S11 and A11) can also be considered a contributing factor.

5. Conclusions

An international Round-Robin was conducted among four laboratories (BAM, IMR-TU, NIST and SCK•CEN) in order to characterize the tensile properties of iron with different purity levels, ranging from commercially pure (99.984 %) to ultra-high purity (> 99.999 %). Tensile tests were performed at room temperature and at different strain rates in the range 10^{-5} s^{-1} to 5×10^{-3} s^{-1}. The data collected from the participating labs provide a consistent picture of the investigated materials' tensile properties, as well as of the influence of strain rate and material purity.

The following conclusions can be drawn from the analysis of the Round-Robin results.

(1) As expected, an increase of strain rate causes an increase of yield strength and, to a lesser extent, tensile strength for all the materials. Average test results were fitted by power law relationships, showing that the strain rate sensitivity (quantified by the regression exponent) increases with material purity. The effect of strain rate is most pronounced for ultra-high-purity iron (A11).

(2) Yield and tensile strength clearly decrease with increasing material purity. Ductility is similarly affected, although once again trends are less well-defined.

(3) A clear difference in tensile properties was observed between the two high-purity materials (K02 and S11), caused by differences in chemical composition and in the production process.

Acknowledgments

The collaboration of Jeff Sowards and David McColskey at NIST Boulder is gratefully acknowledged, as well as the many fruitful discussions and the technical review of this report.

References

[1] K. Abiko, T. Nakaima, N. Harima, and S. Takaki, "*Preparation of 10 kg Ingot of Ultra-Pure Iron*," Phys. Stat. Sol. (a) **167** (1998), pp. 347-355.

[2] S. Takaki and K. Abiko, "*Ultra-Purification of Electrolytic Iron by Cold-Crucible Induction Melting and Induction-Heating Floating-Zone Melting in Ultra-High Vacuum*," Materials Transactions, JIM, Vol. 41, No. 1 (2000), pp. 2-6.

[3] K. Abiko, "*Iron, Ultrahigh-purity*" in "Encyclopedia of Materials: Science and Technology", Second Edition, Elsevier Publishing, 2002, pp. 1-9.

[4] B. Rehmer, "*BAM Test report: Round Robin Tensile Strength Test of Pure Iron*," BAM 5.2, 2014-12-10.

[5] J. F. Alder and V. A. Philips, "*The effect of strain rates and temperature in the resistance of aluminium, copper and steel to compression*," Journal of Applied Physics, Vol. 15 (1954), pp. 22-32.

[6] N. NagarajaRao, M. Lohrmann, and L. Tall, "*Effect of strain rate on the yield stress of structural steel*", ASTM Journal of Materials, Vol. 1, No. 1, March 1966, Publication No. 293.

[7] E. El-Magd, "*Mechanical properties at high strain rates*," Journal de Physique IV, 1994, 04 (C8), pp.C8-149-C8-170.

[8] "*The Behaviour of Carbon Steels at High Strain Rates and Strain Limits*," Health & Safety Executive, Offshore Technology Report - OTO 1999 018, October 1999.

[9] R. W. Armstrong and S. M. Walley, "*High strain rate properties of metals and alloys*," International Materials Reviews, Vol. 53, No. 3, 2008, pp. 105-128.